DYNAMIC LONGITUDINAL RESPONSE OF A BURIED CAVITY OF CIRCULAR CROSS SECTION

A.R. Carriveau, J.M. Zanetti and R.B. Edwards

SYNOPSIS

The longitudinal dynamic response of a two-dimensional cavity imbedded in an elastic half-space subjected to plane, horizontally polarized shear waves has been studied using an integral equation formulation. The response on the cavity surface is found in terms of a steady-state response ratio with the response of the free surface. Results are presented for several different angles of incidence in the exciting plane wave. Also, a shallow, intermediately deep, and deep cavity are studied to examine the effect of depth. Comparisons are made between the diffracted displacement field on the cavity and the incident, undiffracted field. At very low frequencies, that is waves whose length are large compared to cavity dimensions, diffraction effects are minimal. This suggests that for most applications, the incident field very closely approximates that which considers the diffraction effects.

RESUME

Dans cet article, on présente les résultats d'une étude sur la réponse dynamique d'une cavité souterraine plane, sise dans un espace élastique soumis à des ondes de cisaillement planes et horizontales. On a étudié plusieurs angles d'incidence de l'onde excitatrice de même que l'effet de la profondeur de la cavité. On a comparé le champ des déplacements diffractés sur la cavité au champ incident non diffracté. A basses fréquences, c'est-à-dire lorsque la longeur des ondes est grande comparée aux dimensions de la cavité, les effets de la diffraction sont minimes. Par conséquent, pour la plupart des applications, le champ incident ressemble beaucoup au champ diffracté.

A. R. Carriveau is a Senior Engineer employed at URS/John A. Blume & Associates, Engineers, since 1976. He has specialized in the fields of theoretical ground motion synthesis and dynamic soil-structure interaction. He holds B.S., M.S., and Ph.D. degrees from the University of California, Los Angeles, and is a member of the American Society of Civil Engineers and the Seismological Society of America.
R. B. Edwards is presently an Associate Seismologist with URS/Blume. Mr. Edwards received a B.S. in Physics from Worcester Polytechnical Institute and an M.A. in Geophysics from the University of California, Berkeley. He participated in the development of seismic design criteria for underground structures for the U.S. Department of Energy and the National Science Foundation.
J. M. Zanetti is presently Senior Seismologist with URS/Blume. Mr. Zanetti obtained a B.S. in Physics from Fairfield University and an M.S. in Geophysics from the University of California, Berkeley. He has participated in the development of ground motion design criterion for surface and underground structures for the U.S. Department of Energy and the National Science Foundation. He is a member of the Seismological Society of America.

INTRODUCTION

In recent years, there has been much interest in the underground siting of critical installations in seismically active areas. This necessitates consideration of the effects of seismic waves on such installations to guard against the failure of the host medium in the vicinity, to design the tunnel lining against overstressing, and to predict the shaking of the contents to adequately safeguard against damage. Observations of shaking effects and damage to many different kinds of underground facilities suggest seismic waves are much less damaging to them than to surface structures. However, a paucity of strong motion data in and around underground installations requires an analytical approach rather than an empirical one. Suitable, simple, mathematical models of the underground installation, the surrounding earth and the seismic wave excitation, that retain the physical subtleties and that can be applied to real situations, are needed. Thus it is important to study various applicable models leading to better understanding of the phenomenon.

This study deals with the dynamic response of a two dimensional cavity in an elastic half-space. The cavity is of circular cross section. Its axis lies at a finite distance from and parallel to the free surface of the half-space. The seismic excitation is represented by a plane, horizontally-polarized shear wave of arbitrary angle of incidence. Its displacement component is parallel to the infinite dimension of the cavity and, of course, parallel to the free surface. This is schematically shown in Figure 1. The plane wave and cavity response have harmonic time dependence.

The displacement response of the cavity is related to the displacement response of the free surface in the absence of any cavity in the medium. This response is expressed as a frequency dependent ratio depending on two dimensionless parameters: the angle of incidence of the impinging wave, and the depth to radius ratio of the cavity. Having determined this response ratio for appropriate values of these parameters, arbitrary ground motion is easily handled by Fourier synthesis.

A large number of excellent papers, treating the scattering of plane seismic waves by cylindrical holes and rigid inclusions, have appeared in the literature; however, no studies have been reported on the scattering of seismic waves by scatterers embedded in a half-space. The scattering of compressional waves by a rigid cylinder in a full space was studied by Gilbert and Knopoff (1). They obtained the exact solution in integral form, which they evaluated asymptotically for an estimate of first motions. Gilbert (2) presented the scattering of P, SV, and SH waves by a cavity of circular cross section in a full space similarly looking at first motions. Banaugh and Goldsmith (3) studied the scattering of plane steady-state acoustic waves by cavities of arbitrary shape embedded in a full space using an integral equation formulation. The transient response of an elastically lined circular cylinder in a full space excited by a plane compressional wave was given by Garnet and Crouzet-Pascal (4). In a very thorough study, Mow and Pao (5) treat both transient and steady-state diffraction problems of all wave types by various scatterer configurations, and using all the different solution techniques. Their work also contains an excellent bibliographic review of previously published studies.

Other studies worthy of mention include a very recent paper by Niwa et al (6) which deals with the transient stresses around a tunnel, lined or unlined, using the integral equation method. They obtain a good comparison with the results of Garnet and Crouzet-Pascal (4). This paper also treats the full space problem as do all the previously cited works. There are publications by Dowding and Rozen (7) and Rozen (8) presenting the results of earthquake damage surveys. Glass (9) summarizes previous closed form solutions for lined circular cavities and uses the finite element method to extend these analyses to adjacent unlined cavities. Finally, other studies have been performed at the University of Illinois at Urbana, for example, Yoshihara et al (10), which were not available for review by this time. The above-mentioned publications are not a complete bibliographic review, but they serve to highlight the background for this study.

The integral equation method was chosen herein to evaluate the response of the two dimensional cavity. The integral equation has been formulated by use of the appropriate form of the Green's function for the half-space, thereby satisfying the stress-free conditions on both the free surface of the half-space and on the surface of the cavity. The integral equation is discretized, casting it in a matrix form of a system of linear equations with complex coefficients. The system is solved for impinging plane waves of several angles of incidence. Although not done in this investigation, this procedure is readily adaptable to lined cavities of arbitrary shape.

FORMULATION OF THE PROBLEM

Consider the displacement field in the half-space as excited by a plane, horizontally polarized shear wave of angle of incidence θ measured between the normal to the wave front and the outward normal to the free surface at $x_2 = 0$. The total incident displacement in the half-space due to this wave and the reflected wave from the free surface can be given by

$$U_3^i(x_1, x_2; \omega) = U_3^o(\omega) \cos\left(\frac{\omega}{\beta} x_2 \cos\theta\right) e^{-i\frac{\omega}{\beta} x_1 \sin\theta} \tag{1}$$

where ω is the circular frequency of the exciting plane wave; β is the shear wave velocity in the half-space; x_1 and x_2 are the horizontal and vertical Cartesian coordinates, respectively, as shown in Figure 1; i is the imaginary number equal to $\sqrt{-1}$; and $U_3^o(\omega)$ is the Fourier transform of the displacement time history in the absence of the cavity as observed at the point 0, designated as the origin of coordinates ($x_1 = 0$, $x_2 = 0$). The exciting wave is propagating to the left in the positive sense of x_1. The time dependence used herein is $e^{i\omega t}$.

The cavity, of radius r_o, is located with its center at depth $x_2 = d$ from the free surface. Notice that the cavity center is directly beneath the point 0.

Introducing a cylindrical polar coordinate system whose origin is at the cavity center, let the relation to the original Cartesian system be given by

$$x_1 = \sin\psi \tag{2}$$

$$x_2 = d + r\cos\psi \tag{3}$$

in which the polar angle ψ is measured clockwise starting from the x_2-axis as shown in Figure 2, and r is the polar distance given by

$$r = \sqrt{x_1^2 + (x_2 - d)^2} \tag{4}$$

Using these new coordinates, the incident wave field, given in Equation (1), can be expressed alternately by

$$U_3^i(r, \psi; \omega) = U_3^o(\omega) \cos\left(\frac{\omega}{\beta} \cos\theta \, [d + r\cos\psi]\right) e^{-i\frac{\omega}{\beta} r \sin\psi \sin\theta} \tag{5}$$

Introducing the appropriate form of the Green's function for this problem, it is given in the Cartesian coordinates by

$$G_{33}(x_1, x_2, \xi_1, \xi_2, \omega) = \frac{-i}{4\mu}\left[H_o^{(2)}\left(\frac{\omega}{\beta}\sqrt{(x_1 - \xi_1)^2 + (x_2 - \xi_2)^2}\right) + H_o^{(2)}\left(\frac{\omega}{\beta}\sqrt{(x_1 - \xi_1)^2 + (x_2 + \xi_2)^2}\right)\right] \tag{6}$$

where μ is the shear modulus of the half-space; ξ_1 and ξ_2 are the coordinates of the source point and $H_o^2(Z)$ is the Hankel function of zero order, second kind of argument Z. Specifically, Equation (6) gives the displacement component in the direction 3 at point (x_1, x_2) due to

a line force acting in direction 3 at (ξ_1, ξ_2) for the harmonic component of frequency ω. Notice that the second Hankel function in Equation (6) gives the contribution from an image source representing the effect of the free surface at $x_2 = 0$.

Using the new coordinates, the Green's function given in Equation (6) can be rewritten as

$$G_{33}(r, \psi, \rho, \eta; \omega) = \frac{-i}{4\mu}\left[H_o^{(2)}\left(\frac{\omega}{\beta} R\right) + H_o^{(2)}\left(\frac{\omega}{\beta} R^*\right)\right] \tag{7}$$

in which the source-observation point distance is

$$R = \sqrt{r^2 + \rho^2 - 2r\rho \cos(\psi-\eta)} \tag{8}$$

and the image source-observation point distance is

$$R^* = \left[r^2 + \rho^2 + 2r\rho \cos(\psi+\eta) + 4 r^2\left(1 + \frac{d}{r}\cos\psi + \frac{d\rho}{r^2}\cos\eta\right)\right]^{1/2} \tag{9}$$

The coordinates ρ and η are the source point cylindrical polar radial distance and angle respectively, analogous to r and ψ of the observation point.

The problem of determining the response of the cavity surface, due to any impinging wave, can be found in the solution to the following integral equation, see Mow and Pao (5):

$$U_3^i(r_o, \psi) = \frac{1}{2} U_3(r_o, \psi) - \mu \int_A U_3(r_o, \eta) \frac{\partial}{\partial n} G_{33}(r_o, \psi, \rho = r_o, \eta)\, dA(\eta) \tag{10}$$

where A denotes the surface area of the cavity, and n is the outward normal to the cavity surface. In Equation (10), the frequency ω in the function arguments has been omitted for convenience. The solution of Equation (10), $U_3(r_o, \eta)$, then, is the desired displacement response of the cavity perimeter due to the incident wave $U_3^i(r_o, \psi)$. Equation (10) can be discretized replacing the integral with a sum

$$U_3^i(r_o, \psi_j) = \frac{1}{2} U_3(r_o, \psi_j) + \mu r_o \Delta\eta \sum_{m=1}^{N} U_3(r_o, \eta_m) \frac{\partial}{\partial\rho} G_{33}(r_o, \psi_j, r_o, \eta_m) \tag{11}$$

in which the sum on m replaces the surface integral, the incremental area becomes

$$dA(\eta) = r_o \Delta\eta = r_o \frac{2\pi}{N} \tag{12}$$

and the normal derivative is given by the negative of the radial derivative. This term can be determined from Equation (7) for $m \neq j$ as

$$\mu \frac{\partial}{\partial \rho} G_{33}(r_o, \psi_j, r_o, \eta_m)$$

$$= \frac{i\omega}{4\beta}\left\{\sqrt{\frac{1 - \cos(\psi_j - \eta_m)}{2}}\, H_1^{(2)}\left(\frac{\sqrt{2}\,\omega r_o}{\beta}\sqrt{1 - \cos(\psi_j - \eta_m)}\right)\right.$$

$$+ H_1^{(2)}\left(\frac{\sqrt{2}\,\omega r_o}{\beta}\sqrt{1 + \cos(\psi_j + \eta_m) + 2\left(\frac{d^2}{r_o^2} + \frac{d}{r_o}\cos\psi_j + \frac{d}{r_o}\cos\eta_m\right)}\right)\left[1 + \right.$$

$$\cos(\psi_j + \eta_m) +$$

$$\left.\left. 2\frac{d}{r_o}\cos\eta_m\right] \Big/ \left[\sqrt{2}\sqrt{1 + \cos(\psi_j + \eta_m) + 2\left(\frac{d^2}{r_o^2} + \frac{d}{r_o}\cos\psi_j + \frac{d}{r_o}\cos\eta_m\right)}\right]\right\} \qquad (13)$$

and for m = j after using the appropriate asymptotic form for the Hankel function

$$\mu \frac{\partial}{\partial \rho} G_{33}(r_o, \psi_j, r_o, \eta_j) = \frac{i\omega}{4\beta}\left\{\frac{i\omega}{\pi\omega r_o} + \right.$$

$$H_1^{(2)}\left(\sqrt{2}\,\frac{\omega r_o}{\beta}\sqrt{1 + \cos 2\eta_j + 2\left(\frac{d^2}{r_o^2} + 2\frac{d}{r_o}\cos\eta_j\right)}\right)\left[1 + \cos 2\eta_j\right.$$

$$\left.\left. + 2\frac{d}{r_o}\cos\eta_j\right] \Big/ \left[\sqrt{2}\sqrt{1 + \cos 2\eta_j + 2\left(\frac{d^2}{r_o^2} + 2\frac{d}{r_o}\cos\eta_j\right)}\right]\right\} \qquad (14)$$

Figure 3 graphically depicts the discretization scheme for N = 8.

The incident wave expression of Equation (5) can also be evaluated at the same discretization points. This yields

$$U_3^i(r_o, \psi_j) = U_3^o(\omega)\cos\left(\frac{\omega}{\beta}\cos\theta[d + r_o\cos\psi_j]\right) e^{-i\frac{\omega}{\beta} r_o \sin\psi_j \sin\theta} \qquad (15)$$

Substitution of Equations (13), (14), and (15) into Equation (11) leads to a N x N system of linear equations in $U_3(r_o, \psi_j)$ with complex coefficients.

NUMERICAL EVALUATION

The solution of the set of equations described above was performed using a complex Gaussian elimination procedure. The number of discretization points used varied with the frequency of the wave motion. For values of $\omega r_o/\beta$ between zero and 0.4, 16 points were used in the discretization. In the interval 0.4 to 0.6, 32 points were used. Finally from 0.6 to 1.0, 64 points were used. This scheme was selected to assure a sufficient number of points per wave length especially for the higher frequency range. The accuracy of the discretization technique used here was not studied. This consideration has been reported elsewhere (3,5). The Gaussian elmination solution technique, however, was verified to have an accuracy of 5×10^{-13} compared to 1.0.

RESULTS

The response of the cavity $U_3(r_o,\psi_j)$, as defined by Equation (11), was put in dimensionless form before solution. Dividing it by the Fourier transform of the surface motion $U_3^o(\omega)$ leads to a system of equations in the response ratios for the discretization points on the circumference of the circle to the origin point above on the free surface. This division conveniently removes the dimensionality of Equation (11). Thus, the solution has been generalized for any arbitrary time dependence associated with the incident wave. A spectral multiplication of the response ratio for the point on the cavity surface with the Fourier transform of the time history to be assigned to the surface motion results in the Fourier transform of the response of that point. A Fourier inversion yields the corresponding response time history.

The response ratio obtained in the solution of the discretized integral equation is for a particular value of the frequency. The system of equations was repeatedly reconstructed and solved for a number of different frequency values permitting a reasonably smooth response curve to be plotted. As an example of the kind of results obtained therein, Figure 4 shows the response ratio values around the circumference of the circle for four different angles of incidence of the impinging wave. Both the real and imaginary parts are displayed, inward towards the circle center being a positive value. The frequency, expressed in a dimensionless form as

$$\Omega = \omega r_o/\beta \tag{16}$$

for the response depicted in Figure 4, has the value 0.4. The depth to radius ratio, d/r_o, is 6. Notice that for 0° angle of incidence the cavity response is symmetric about the vertical centerline as should be expected. As the angle of incidence changes to a more horizontally impinging wave the response becomes more symmetric about the horizontal centerline, although it never achieves this symmetry because of the influence of the reflected wave from the free surface. For the 90° angle, the real part appears fairly symmetric across the horizontal centerline; whereas the zero crossing of the imaginary part is clearly shifted from the vertical line passing through the circle's center.

Figure 4 also shows the completeness of the solution obtained from the integral equation method used in this work. The response of all points around the circumference of the cavity are obtained as the system of equations is solved. This is a very desirable feature of the method since the response point of interest may depend on the particulars of the application.

Figure 5 presents response ratios for the point on the cavity bottom. These are displayed versus the dimensionless frequency Ω defined in Equation (16). Three depth to radius ratios are shown, namely: 6, 20, and 100. These represent a shallow, intermediately deep, and a deep cavity. The results for four angles of incidence, 0°, 30°, 60°, and 90°, are plotted. The range of dimensionless frequency for which the ratios have been displayed is between zero and 1.0 for the depth

to radius ratios of 6 and 20. For the depth to radius ratio of 100, the dimensionless frequency range is between zero and 0.1. This different range in the latter case was chosen because, at the same scale, the curves would be very difficult to distinguish due to their many oscillations. The behavior of the curves are clearly seen as plotted. Notice that the imaginary parts amplitudes of these first two response ratios increase slowly from negligibly small values near zero frequency to significant values in the vicinity of $\Omega = 1$. The imaginary part, on the other hand, for the deep cavity $d/r_o = 100$, is negligible, less than 0.01 in the range shown. For this reason, it was not plotted.

For most applications the dimensionless frequency range $0 \leq \Omega \leq 1.0$ should be adequate. For example, for tunnels of radius 10 feet or less in a medium with a shear wave velocity of greater than about 700 feet per second, the circular frequency range $0 \leq \omega \leq 20\pi$ will be covered. This frequency range incorporates most of the significant frequency content in recorded strong motion accelerograms. For smaller tunnel radius or for larger shear wave velocity, this frequency range will be extended considerably. The 700 feet per second shear wave velocity is surely very low for rock-type earth material in which an unlined tunnel could be constructed.

Examination of the diffraction of the SH wave around the cavity is also of interest in this study. To this end, a comparison is made between the response at the bottom of the cavity and the motion at that same point in the absence of the cavity. This undiffracted field is given by Equation (1) in which $x_1 = 0$, and $x_2 = d+r_o$. Of course, as in the previous treatment, Equation (1) is first normalized by dividing by the quantity $U_3^0(\omega)$. This results in the cosine factor remaining as defining the unscattered field at that point. This represents both the incident plane wave front and the front reflected from the free surface. Figure 6 gives the comparison between this normalized incident field and the cavity bottom response which includes scattering versus the dimensionless frequency Ω. Two angles of incidence are shown, 0° and 60°, for two depth-to-radius ratios 6 and 20. In all cases, at low frequencies the incident field is very close to the field which includes scattering. The curves slowly diverge as the frequency increases. Even as the frequency approaches 1.0, the incident field curves are fairly close to those including scattering. The difference shown here between these curves is due to the effect of scattering. It should be noted that the imaginary part of the incident field is identically zero. Thus, a comparison between it and the imaginary part of the response ratios in Figure 5 has not been made. The same comparison for the deep cavity of depth to radius ratio of 100 was also made. However, these results were not shown on this figure because the difference between the incident and scattered field was so slight that they could not be distinguished in a plot. Then, for practical purposes it can be concluded that in the frequency range $0 \leq \Omega \leq 0.1$ the incident and diffracted field are the same for this case.

DISCUSSION

The comparison in Figure 6 suggests that the cavity response can be quickly estimated in the low frequency range by the incident wave field. This is indeed true for the deep case, $d/r_o = 100$, displayed here. For the other two cases, this suggested estimation procedure is still valid for the low frequency range. How far out on the frequency scale that this estimate can be used, will depend on the acceptable error. The divergence between these curves in Figure 6, then, are a measure of this error. Scanning the curves, and deciding the frequency beyond which the difference is unacceptable will define the acceptable low frequency approximation range. Using the incident field will, however, never yield an imaginary part. Recovering an estimate for it requires higher order approximation techniques. These will not be considered in this study.

Other response quantities in this problem that are frequently of interest are the shear stresses or strains in the medium around the cavity. These have not explicitly been obtained in this study. They can be found, for example, using a finite difference scheme from the discretized response that has been evaluated.

A distinct advantage of the steady-state formulation by the integral equation method, with the subsequent numerical solution, is that the earth material surrounding the cavity can readily be made visco-elastic by the addition of a frequency dependent imaginary part to the material modulus. The choice of frequency dependence will correspond to a particular material damping mechanism. The usual dependence chosen for earth materials is a small constant, independent of frequency which is the functional form for constant hysteretic damping. Incorporation of this feature will not conceptually change either the formulation or solution technique. It does introduce a complex shear wave velocity which requires the evaluation of the Hankel functions for complex arguments. The discretization and resulting system of linear equations can be handled in the same manner as already described for the case without visco-elasticity. Another important advantage of the integral equation method is that the radiation of the scattered wave field is correctly incorporated in the solution through the use of the Green's function. This contrasts the inability of lumped parameter methods, such as finite element or finite difference, which model a region around the cavity with finite elements or a finite difference grid to some distance away. These methods have a built-in difficulty with the radiation of the scattered field as it tends to be reflected back from the outer boundaries of the modelled region to the vicinity of the cavity thereby contaminating the response of the area under scrutiny. Moreover, these methods usually do not have a built-in mechanism to specify the excitation as an arbitrary wave form easily described in seismological terms. The wave form in the formulation used here is built-in and does not add to the difficulty of the problem or its solution. Another disadvantage of the finite element and finite difference methods is that they use a transient technique in which a particular time dependence must be assigned to the excitation. This means that the solution procedure must be repeated for different time dependent excitation forms. With the steady-state method used here,

Fourier synthesis can provide for arbitrary time dependence in the incident wave as already discussed.

CONCLUSION

The problem of a buried circular cavity in half-space subjected to horizontally polarized shear waves of arbitrary angle of incidence has been studied. The steady-state response of the cavity expressed in terms of the free surface motion has been evaluated for a shallow, intermediate and deep cavity. Four angles of incidence have been considered for the excitation giving the effect of the full variation of this parameter. Comparisons between the response of the cavity including diffraction and the incident wave field, which represent the motion without these effects, have been presented. These comparisons suggest that for low frequencies, the diffraction effects are small, and cavity response can be estimated by the incident, unscattered motion.

Future research in this field should include examination of damping in the earth medium, lining on the cavity, and an arbitrary shape for the cavity cross section. Also, the problems of compressional and in-plane shear wave excitation of arbitrary angles of incidence, and Rayleigh waves, should be investigated.

ACKNOWLEDGMENTS

The authors gratefully acknowledge the support of this research by the National Science Foundation Grant No. PFR 77-06505, partially funded by the Federal Highway Administration, Department of Transportation. The authors also thank Dr. Debabrata Ray for his timely assistance in the implementation of the integral equation solution.

REFERENCES

1. Gilbert, F. and Knopoff, L., "Scattering of Impulsive Elastic Waves by a Rigid Cylinder," Journal of the Acoustical Society of America, Vol. 31, No. 9, Sept. 1959, pp. 1169-1175.

2. Gilbert, F., "Scattering of Impulsive Elastic Waves by a Smooth Convex Cylinder," Journal of the Acoustical Society of America, Vol. 32, No. 7, July 1960, pp. 841-857.

3. Banaugh, R.P. and Goldsmith, W., "Diffraction of Steady Acoustic Waves by Surfaces of Arbitrary Shape," Journal of the Acoustical Society of America, Vol. 35, No. 10, Oct. 1963, pp. 1590-1601.

4. Garnet, H. and Crouzet-Pascal, J., "Transient Response of a Circular Cylinder of Arbitrary Thickness, in an Elastic Medium, to a Plane Dilatational Wave," ASME Journal of Applied Mechanics, Vol. 33, Sept. 1966, pp. 521-531.

5. Mow, C.C. and Pao, Y.H., "Diffraction of Elastic Waves and Dynamic Stress Concentrations," U.S. Air Force Project Rand, R-482-PR, April 1971, 681 pp.

6. Niwa, Y., Kobayashi, S., and Fukui, T., "Applications of Integral Equation Method to Some Geomechanical Problems," Proceedings of ASCE Conference on Numerical Methods in Geomechanics, Vol. 1, June 1976, pp. 120-131.

7. Dowding, C.H. and Rozen, A., "Damage to Rock Tunnels from Earthquake Shaking," Journal of the Geotechnical Division, Vol. 104, Feb. 1978, pp. 175-191.

8. Rozen, A., "Response of Rock Tunnels to Earthquake Shaking," Master of Science Thesis in Civil Engineering, MIT, Cambridge, 1976, 238 pp.

9. Glass, C.E., "Seismic Consideration in Siting Large Underground Openings in Rock," Ph.D. Thesis, Univ. of California, Berkeley, 1976.

10. Yoshihara, T., Robinson, A.R., and Merritt, J.L., "Interaction of Plane Elastic Waves with an Elastic Cylindrical Shell," Department of Civil Engineers, University of Illinois, Technical Report No. SRS 261, Jan. 1963.

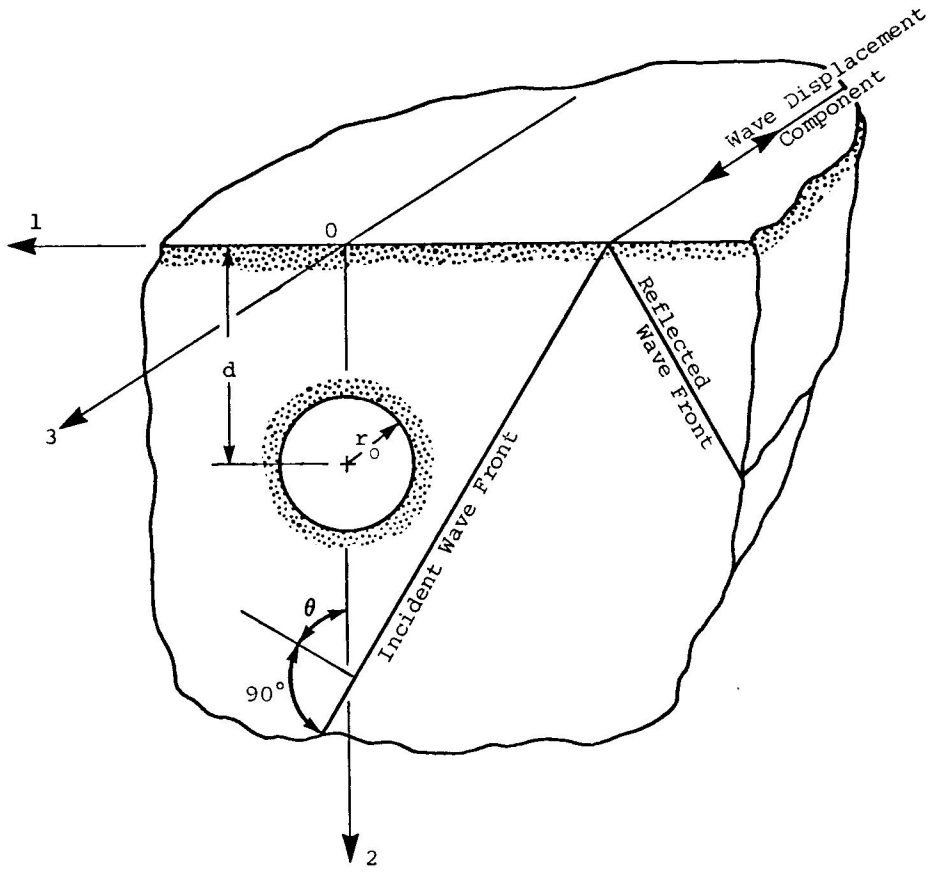

1. The cavity, coordinates and excitation.

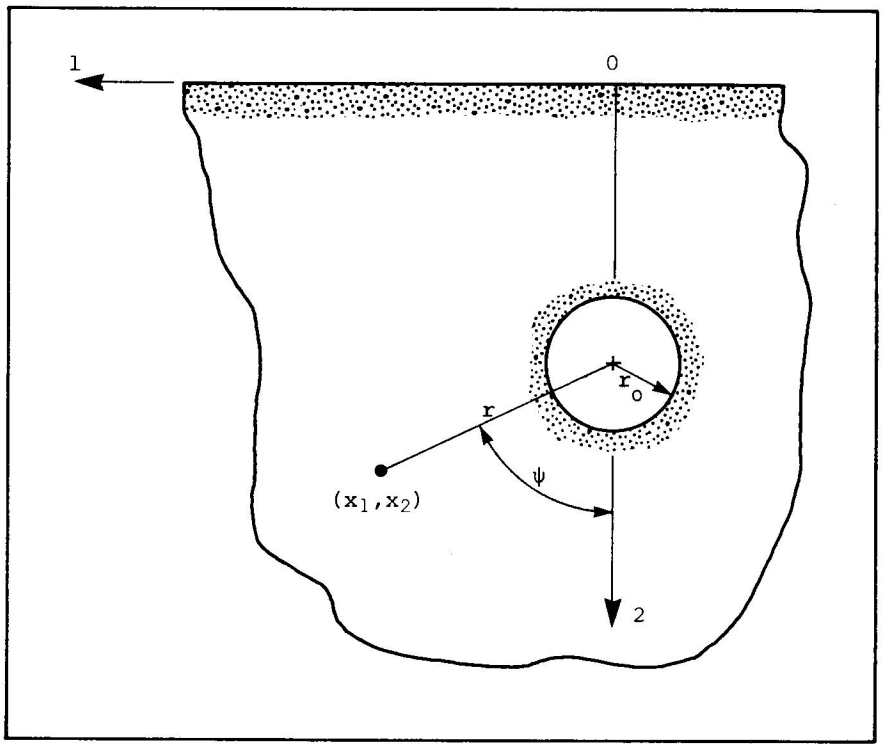

2. Relation between Cartesian coordinates and cylindrical polar coordinates.

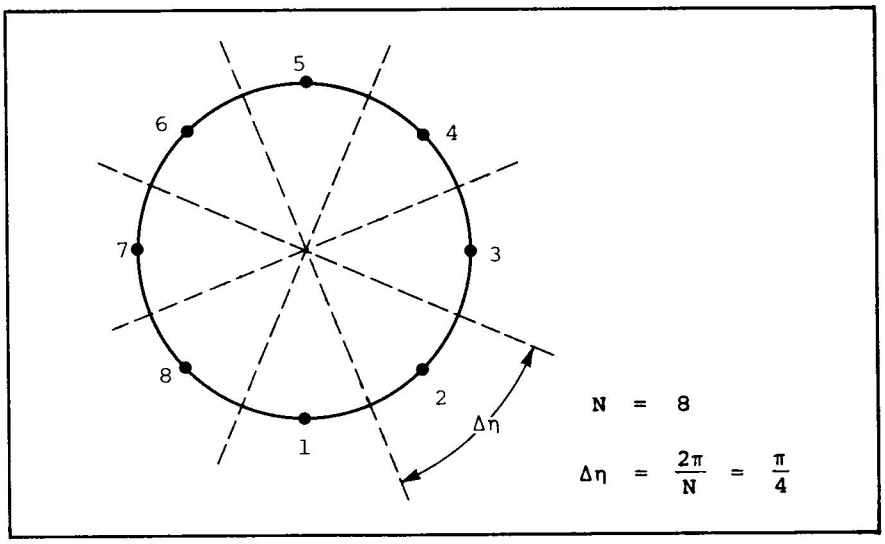

3. Discretization scheme for 8 points.

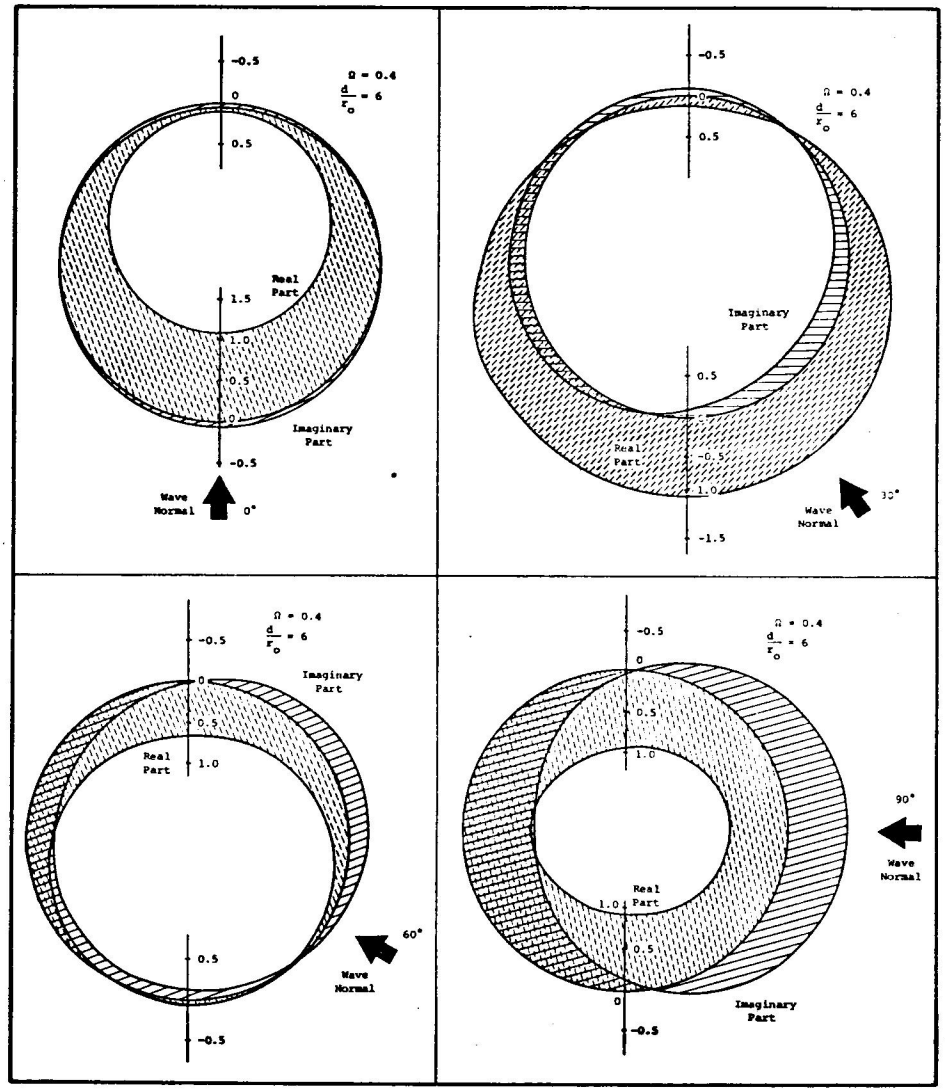

4. Effect of angle of incidence on cavity response ratio on its circumference.

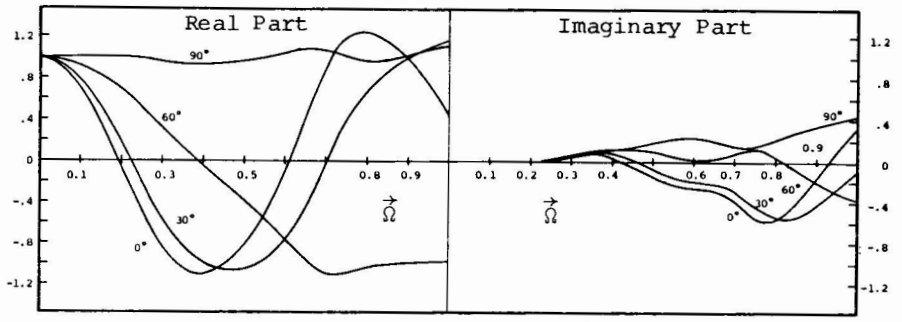

a) Depth to radius ratio, $\frac{d}{r_o}$, is 6.

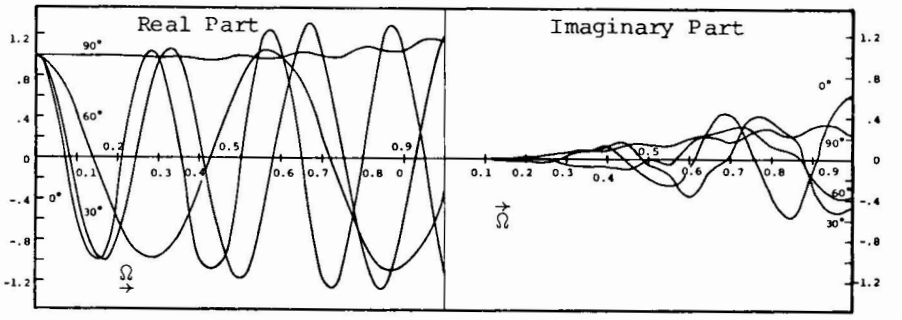

b) Depth to radius ratio, $\frac{d}{r_o}$, is 20.

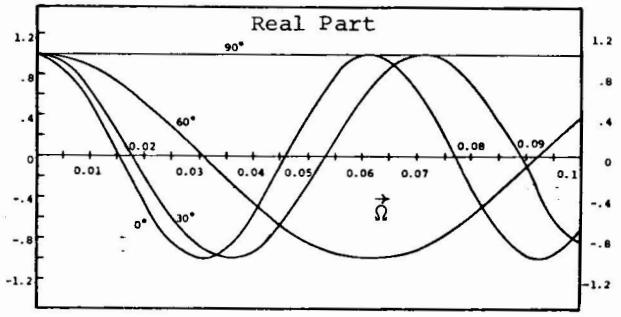

Note: Imaginary part for $\frac{d}{r_o}$ = 100 is less than 0.01 for $0 \leq \Omega \leq 0.1$

c) Depth to radius ratio, $\frac{d}{r_o}$, is 100.

5. Steady-state cavity bottom response ratio to free surface response.

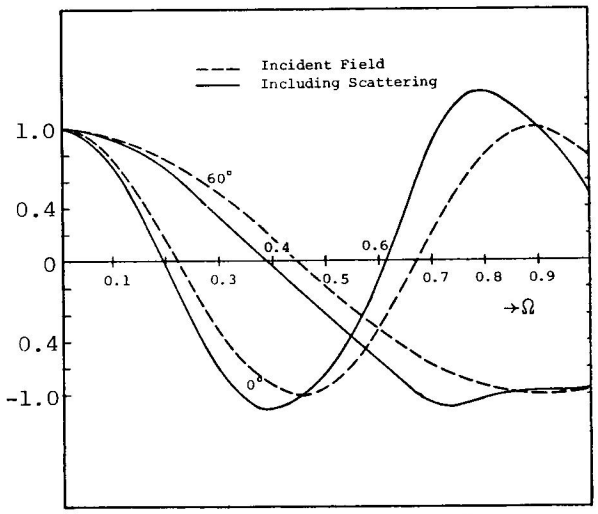

a) Depth to radius ratio, $\frac{d}{r_o}$, is 6.

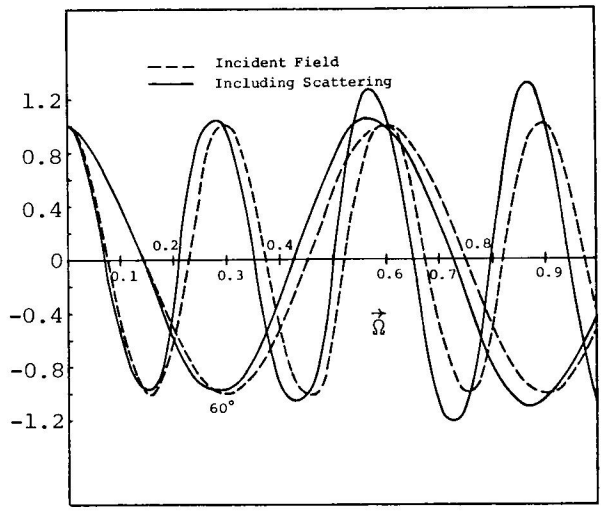

b) Depth to radius ratio, $\frac{d}{r_o}$, is 20.

6. Comparison between motion at cavity bottom and incident wave field in the absence of the cavity.